

Effects of abiotic processes on the correlation between pH and pO₂ in the Norwegian Sea: Implications for GCS monitoring

Christian Totland^{*}, Espen Eek, Raoul Wolf, Ivar-Kristian Waarum, Ann Elisabeth Albright Blomberg

Norwegian Geotechnical Institute, Sandakerveien 140, Sognsveien 72, 0806, Oslo 0484, Norway

ARTICLE INFO

Keywords:

Carbon capture and storage
Geological carbon storage
CO₂ leakage
carbonate system
Norwegian Sea
pH

ABSTRACT

In the absence of abiotic sources of CO₂, variation in pCO₂ and pO₂ is expected to be inversely correlated in the water column due to biogenic processes. It has previously been suggested to use this correlation for leakage monitoring of offshore geological carbon storage (GCS) sites. In this study the aim is to investigate the extent of this correlation in ocean water masses with different origin and history in the Norwegian Sea, as well as in water masses in the vicinity of an active hydrothermal vent field at Mohn's Ridge, where pH is used as a proxy for pCO₂. Over a hydrothermal vent site, a strong correlation between pH and pO₂ is observed from 0 to 1700 m, whereas at depths >1700 m there is no correlation, likely due to CO₂ emissions from the hydrothermal vents. However, at a reference site nearly 200 km from the hydrothermal vents, the intermediate Arctic water masses (700 – 1600 m depth) also show pH-pO₂ correlations that are inconsistent with biogenic processes, but less pronounced compared to the hydrothermal vent site. These findings show that the suitability of this monitoring strategy will depend on a thorough site-specific evaluation of pH/CO₂ and O₂ relationships of relevant water masses.

1. Introduction

In most water masses, variation in pCO₂ and pO₂ is to a large extent determined by processes where CO₂ and O₂ are on opposite sides of the chemical equations, describing biogenic carbon cycling processes. The biogenic processes include degradation of organic matter, in which O₂ is consumed and CO₂ produced, and vice versa for photosynthesis. Since the latter occurs in the euphotic zone at shallower depths, in contrast to degradation processes, pCO₂ is expected to increase with increasing depths. However, regardless of depth, pO₂ and pCO₂ are expected to be inversely correlated in the absence of any other source of CO₂ (Bickle, 2009; Ohtaki et al., 1993; Martinez-Cabanas et al., 2021; Totland et al., 2020; Uchimoto et al., 2017, 2018). This knowledge is important for the marine chemistry modeling and monitoring associated with ocean carbon mitigation strategies, such as deep ocean CO₂ storage (Caldeira and Wickett, 2005), and offshore geological carbon storage (GCS) (Bickle, 2009; Blackford et al., 2017; Martinez-Cabanas et al., 2021; Totland et al., 2020; Uchimoto et al., 2018). The pCO₂-pO₂ correlation is a potential chemical signature that can be used to monitor and detect introduction of CO₂ from abiotic sources to the water column, such as

leakage of CO₂ from offshore GCS reservoirs (Blackford et al., 2017; Totland et al., 2020; Uchimoto et al., 2017, 2018). There will be significant spatial and temporal natural variation in pCO₂ and pH at a given site. Therefore, proposed monitoring approaches based on one parameter, such as the C_{seep} method where water carbon levels are monitored (Omar et al., 2021), require a thorough baseline investigation to quantify and correct for the natural variability. Since the pCO₂-pO₂ correlation is expected to persist despite this natural variation, a monitoring strategy based on these parameters may be less dependent on baseline data.

However, there are few reports on the extent of pO₂-pCO₂ correlation for different ocean water masses which consider the influence of natural abiotic CO₂, such as emissions from the earth's crust. We have previously monitored the pCO₂-pO₂ and pH-pO₂ correlation over the course of one month at 60 m depth in the Oslo Fjord (Totland et al., 2020), and found that the correlation persisted despite introduction of new water masses at the site. In that experiment, constructed CO₂ leakage scenarios were detected by disruptions in the pCO₂-pO₂ and pH-pO₂ correlations, even when elevated pCO₂ or reduced pH levels did not exceed the ambient variation. Uchimoto et al. (2017, 2018) made similar

^{*} Corresponding author.

E-mail address: Christian.totland@ngi.no (C. Totland).

<https://doi.org/10.1016/j.ijggc.2023.103879>

Received 5 December 2022; Received in revised form 22 February 2023; Accepted 1 April 2023

Available online 4 April 2023

1750-5836/© 2023 The Authors. Published by Elsevier Ltd. This is an open access article under the CC BY license (<http://creativecommons.org/licenses/by/4.0/>).

observations in the Osaka Bay at 20 m depth, also when monitoring over one full year to capture effects of seasonal variations (Uchimoto et al., 2021).

In this study the aim is to investigate the extent of this correlation in ocean water masses with different origin and history in the Norwegian Sea, as well as in water masses in the vicinity of active hydrothermal vent fields. Similar to a hypothetical leaking offshore CO₂ reservoir, such vents are abiotic sources of CO₂ into the water column. Hence, this knowledge can be useful for the planning and design of monitoring programmes for GCS. Moreover, knowledge of the marine chemistry of the ocean currents, and the marine carbonate system, is important for determining air-sea CO₂ exchange, where ocean biogeochemistry and climate models are closely linked (Burd et al., 2015; Humphreys et al., 2018; Lønborg et al., 2020).

The Norwegian Sea is composed of different water masses originating in the Arctic and Atlantic oceans with associated currents (Fig. 1). The warmer and salty upper water layer (ca. 0–500 m) is the return flow from the North Atlantic to the Arctic, whereas the intermediate water masses originate from the Arctic Ocean and Greenland Sea (Blindheim, 1985, 1990).

The water mass located below ca. 2000 m is a homogeneous water mass characterized by low oxygen levels and little exchange with adjacent water masses (Swift and Koltermann, 1988). This water originates from the Greenland Sea Deep Water and Eurasian Basin Deep Water from the Arctic Ocean.

The exchange of water with the Atlantic Ocean is limited by inflow via the Scotland-Greenland Ridge and export via the Denmark Strait and Iceland-Scotland overflow (Sprintall et al., 2013) (Fig. 1). Whereas the Norwegian Sea is relatively deep, with an average depth of about 2 km, the Scotland-Greenland Ridge is shallow, which creates a natural geographic constraint for the interbasin water exchange at larger depths.

A characteristic feature of the Norwegian Sea floor is the 550 km segment of the Arctic mid-ocean ridge called Mohn's Ridge (Fig. 1). This is an ultraslow-spreading class of ocean ridge that is characterized by intermittent volcanism (Dick et al., 2003). Several active hydrothermal vent fields have been discovered at the ridge (Pedersen et al., 2010a,

2010b).

Due to the low exchange of water below a certain depth, it is possible that the chemical signature of a larger water mass is affected by the extensive hydrothermal vent activity. The high temperatures, pressures and low pH involved in hydrothermal circulation induce several processes, including gasification of organic molecules into CO₂, CH₄ and H₂ (Siskin and Katritzky, 1991), and mineralization of recalcitrant dissolved organic carbon (DOC) (Hawkes et al., 2015).

Hydrothermal vents introduce relatively large amounts of CO₂ into the water masses (Resing et al., 2004), as well as H₂S, ammonia and reduced metals that consume O₂ via oxidation reactions (Pedersen et al., 2010a, 2010b). This can affect the pCO₂ and pH directly, pO₂ through introduction of reduced species and can have additional effects on the local carbonate system, such as accelerated CaCO₃ dissolution due to a reduction in CO₃²⁻ caused by reduced pH.

In this study we investigate the entire water column at a reference site in the Norwegian Sea assumed not to be affected by hydrothermal activity, as well as the water column above a hydrothermal vent field. For the latter site, abiotic processes associated with the hydrothermal activity are expected to affect the pO₂-pH correlation, possibly for a relatively large body of water due to the limited circulation in the deeper waters.

2. Materials and methods

We investigated two sites in the Norwegian Sea using sensors mounted on an Autonomous Underwater Vehicle (AUV) launched from the vessel G.O. Sars; one site with a known hydrothermal vent field at Mohn's Ridge previously discovered by the Norwegian Petroleum Directorate, and one reference site in the Norwegian Basin, approximately 200 km from the Mohn's Ridge site (Fig. 1). The cruise was conducted in June 2019.

Two dives were conducted at each site, referred to as Dives 1–4 (Table 1).

Chemical sensors mounted on the AUV included a Contros Hydro-Flash O₂ sensor, Franatech CH₄ sensor, and an Idronaut Eh-pH sensor. The sensor payload also included a CO₂ sensor that malfunctioned

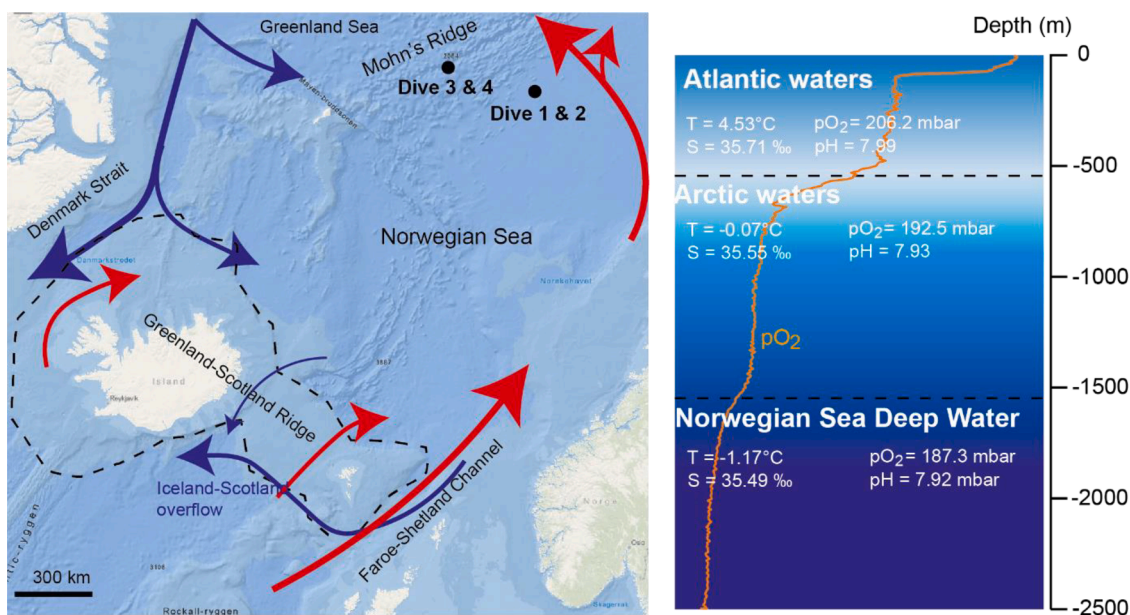


Fig. 1. Left: Map showing the location of Mohn's Ridge and the AUV dive sites. Inflow and overflow branches of Atlantic (red arrows) and Arctic (blue arrows) waters, respectively, are schematically shown. The shallow region of the Greenland-Scotland Ridge is approximately indicated by the dashed line. Right: Characteristics of the water column for the two reference AUV dives in the Lofoten basin of the Norwegian Sea (Dives 1&2). The values for pO₂, S, T and pH are average values for the depth ranges, for both dives. The transition to the Norwegian Sea Deep Water (NSDW) is set based on the depth profile of pO₂ (shown in orange for reference).

Table 1
Description and coordinates for the dive sites.

	UTM33 East	UTM33 North	Description
Dive 1	143,075.7	7,958,449	Reference site (no hydrothermal activity)
Dive 2	144,171.1	7,957,930	Reference site (no hydrothermal activity)
Dive 3	-34,584.4	8,056,757	Known hydrothermal activity
Dive 4	-28,770.3	8,061,590	Known hydrothermal activity

during the first dive. However, ocean pH and $p\text{CO}_2$ are inversely correlated (Totland et al., 2020), and previous studies have shown that reduction in pH around hydrothermal plumes are directly related to the amount of CO_2 released by the vent (Resing et al., 2004). pH is therefore used as a proxy for $p\text{CO}_2$.

The $p\text{O}_2$ and pH sensors have a response time of a few seconds. This contrasts with membrane-based dissolved gas sensors that typically have a relatively long reaction time ($\tau_{63} = 1\text{--}2$ min), which reduce their ability to identify small-scale concentration gradients when mounted on a moving platform such as an AUV (Totland et al., 2020).

The correlation between $p\text{O}_2$ and pH was statistically evaluated assuming segmented linear relationships. For the reference site dives, the occurrence of two breakpoints was assumed *a priori*, while for the plume region dives, one breakpoint was assumed *a priori*. The analysis was performed using the R programming language (R Core Team, 2022) and its add-on package segmented (Muggeo, 2003; 2016; 2017). To account for heteroscedasticity in the covariance matrix of the segmented regression, heteroscedasticity-consistent covariance matrix estimation was performed using functionality from the sandwich add-on package (Zeileis, 2004; 2006; Zeileis et al., 2020). The results of the segmented regression were used to estimate the depth range of the $p\text{O}_2$ breakpoints via linear interpolation between $p\text{O}_2$ and the associated depth values.

3. Results

3.1. Reference site

Fig. 2 shows data acquired during the two dives at the reference site, ca. 200 km from the hydrothermal vent sites. There is a pronounced thermocline from 500 m to about 750 m depth at the reference site (Fig. 2, B and D). The thermocline accompanies a decrease in salinity, which is consistent with the upper waters being the warmer, more salty water flowing in from the North Atlantic Ocean. At the reference site, there is also a small thermocline at 75 m depth, which is common for the deeper regions of the Norwegian Sea (Jones et al., 2019).

Fig. 2A and C further suggest a high degree of correlation between $p\text{O}_2$ and pH in the water masses constituting the upper ca. 670 metres, which is consistent with biogenic CO_2 and O_2 vertical variations. However, the correlation clearly changes at higher depths. This is also illustrated in Fig. 3, where the correlations between pH and $p\text{O}_2$ are given for the various water masses. Between ca. 700 and 1600 m, pH increases with increasing depth, despite a corresponding decline in $p\text{O}_2$. Such an inverse relationship between pH and $p\text{O}_2$ is inconsistent with biogenic degradation of organic matter as this would imply a simultaneous reduction in $p\text{O}_2$ and $p\text{CO}_2$. This intermediate water mass consists of the colder Arctic water.

From ca. 1600 metres the characteristics of the waters change, with decreasing pH and $p\text{O}_2$ values down to the seafloor at ca. 2400 metres. This likely marks the transition down to the Norwegian Sea Deep Water, which is characterized by low oxygen levels and very little exchange with adjacent water masses. However, pH and $p\text{O}_2$ are to some extent correlated in these bottom waters, although with a different slope than in the upper Atlantic waters (Table 2), due to lower variation in oxygen levels.

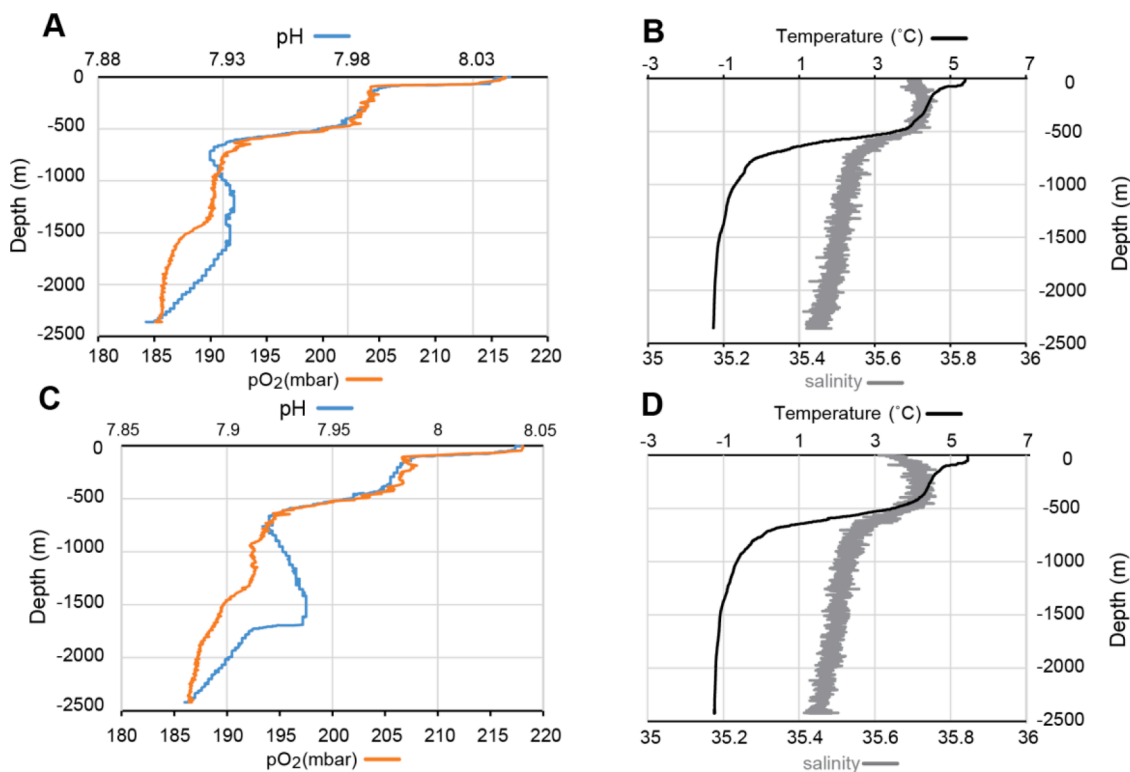


Fig. 2. Data from the two reference site dives, showing pH, $p\text{O}_2$, salinity and temperature for Dive 1 (A and B) and Dive 2 (C and D) as the AUV descended towards the seafloor.

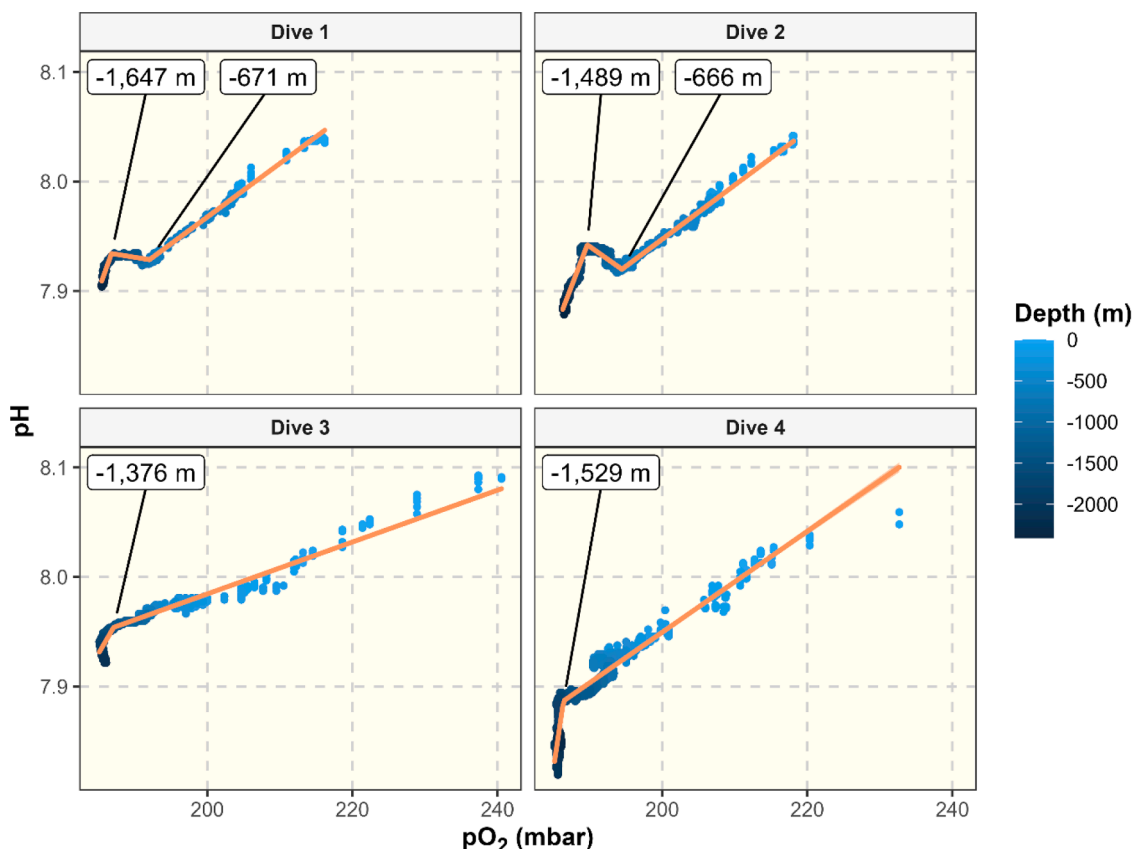


Fig. 3. pH versus pO_2 for reference site dives 1 and 2 (top), as well as plume region dives 3 and 4 (bottom). The results of the segmented linear regression analysis are shown, and labels indicate the depths of the breakpoints. Slopes and adjusted R^2 are given in Table 2. For details, see Materials and Methods.

Table 2

Statistical results from the segmented regression analysis of pO_2 and pH. Based on a regular linear regression, an *a priori* defined segmented relationship was assumed; see Materials and Methods for details. In short, three segments were assumed for dives 1 and 2, and two segments were assumed for dives 3 and 4, resulting in 2 and 1 breakpoint(s), respectively. The predicted breakpoints were used to infer the depths of the breakpoints based on linear interpolation. Values are given as mean \pm standard error.

	Slopes (pH pO_2^{-1})	Breakpoint(s) (pO_2)	Depth(s) (m)	Adjusted R^2
Dive 1	0.019 ± 0.0004	186.8 ± 0.02	-1647 ± 7.5	0.990
	-0.001 ± 0.0006	192.0 ± 0.06	-671 ± 19.7	
	0.005 ± 0.0006			
Dive 2	0.017 ± 0.0001	189.7 ± 0.02	-1489 ± 0.0^a	0.987
	-0.005 ± 0.0002	194.4 ± 0.04	-666 ± 14.0	
	0.005 ± 0.0002			
Dive 3	0.011 ± 0.0006	187.1 ± 0.09	-1376 ± 15.4	0.928
	0.002 ± 0.0008			
Dive 4	0.045 ± 0.0021	186.4 ± 0.08	-1529 ± 0.0^a	0.898
	0.005 ± 0.0030			

^a Determination of a standard error was not possible.

3.2. Hydrothermal vent site

Fig. 4B and D show that the stratification differs at the hydrothermal vent site compared to the reference site. There is a steep thermocline in the upper 250 m, equivalent to the thermocline found at 700 m at the reference site. Moreover, the salinity does not decrease as much near the thermocline and with increasing depths, indicating a more homogeneous water mass which likely originates from the Greenland Sea. Consequently, the data from the reference site are not directly

comparable to those of the hydrothermal site.

In these water masses, pO_2 and pH are well correlated down to ca. 1500–1700 m depths. Below this, the decline in pH with increasing depth is steeper, whereas changes in pO_2 are marginal. Consequently, below these depths, the changes in pH are unrelated to changes in pO_2 which implies that the decline in pH is due to abiotic processes (Figs. 3 and 4). It is reasonable to assume that hydrothermal activity can affect bottom waters; in fact, this is supported by Fig. 4C, where a sharp drop in pH occurs at 1750 m followed by irregular pH variations. During this dive an increase in CH_4 occurs at ca. 2000 m (Fig. 5), showing that the AUV dives directly into a hydrothermal plume. Fig. 4 shows that pO_2 remains unaffected by the fluctuations in pH, indicating that the pH variations are due to the release of CO_2 at the hydrothermal vent field. It is interesting to note that this effect is detectable from the pH- pO_2 correlation more than 700 m from the seafloor (Figs. 4 and 5).

Fig. 6 shows CH_4 and pH variations during the entire dives. For Dive 3, hydrothermal activity is clearly indicated by peaks in methane concentrations as the AUV travels back and forth over the hydrothermal vent site. Negative spikes in pH are also present due to CO_2 plumes created by the vents, although not entirely correlated with the methane spikes. CO_2 is about 100 times more soluble in water at these temperatures than CH_4 . Thus, whereas CO_2 plumes will dissolve quickly in the surrounding water masses, CH_4 plumes may persist for longer, explaining the absence of correlation between the negative spikes in pH and positive CH_4 spikes.

4. Discussion

The results from the reference site (Fig. 2) show that the co-variability of pH and pO_2 at intermediate water depths (ca. 670–1600 m), which correspond to the backflow of cold Arctic waters, is

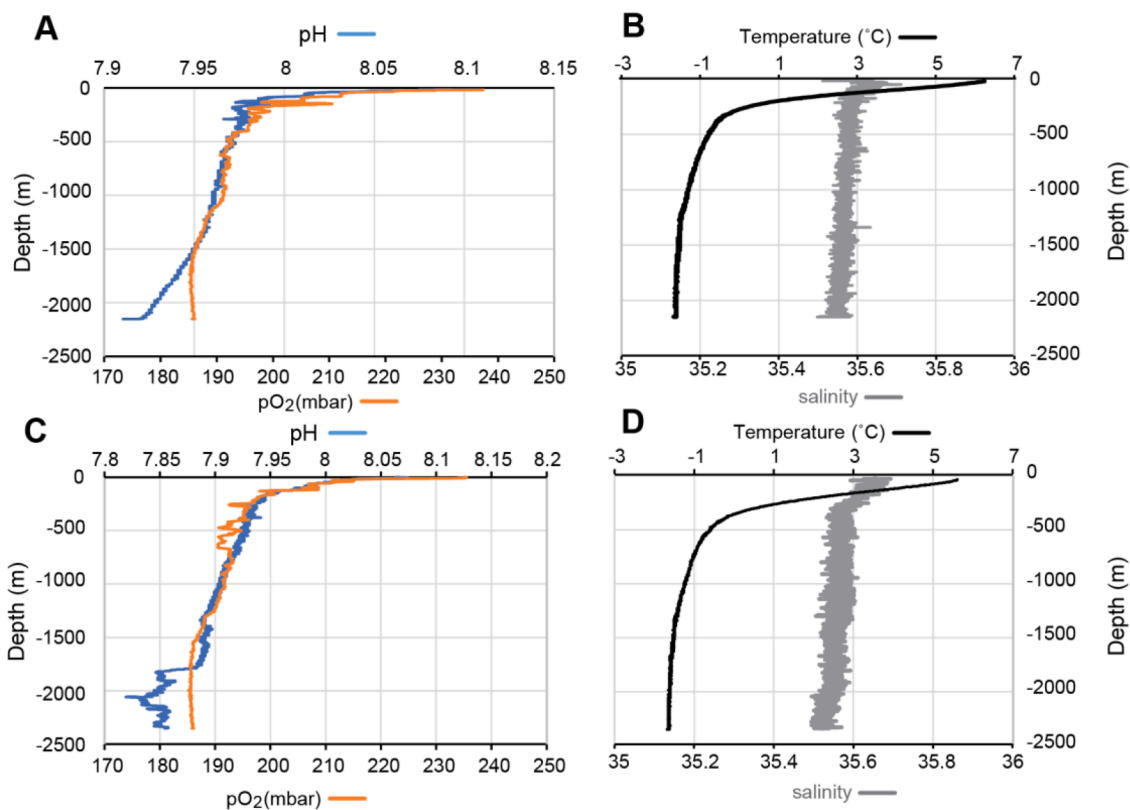


Fig. 4. Data from the two dives at the hydrothermal vent site, showing pH, pO₂, salinity and temperature for Dive 3 (A and B) and Dive 4 (C and D) as the AUV descended towards the seafloor.

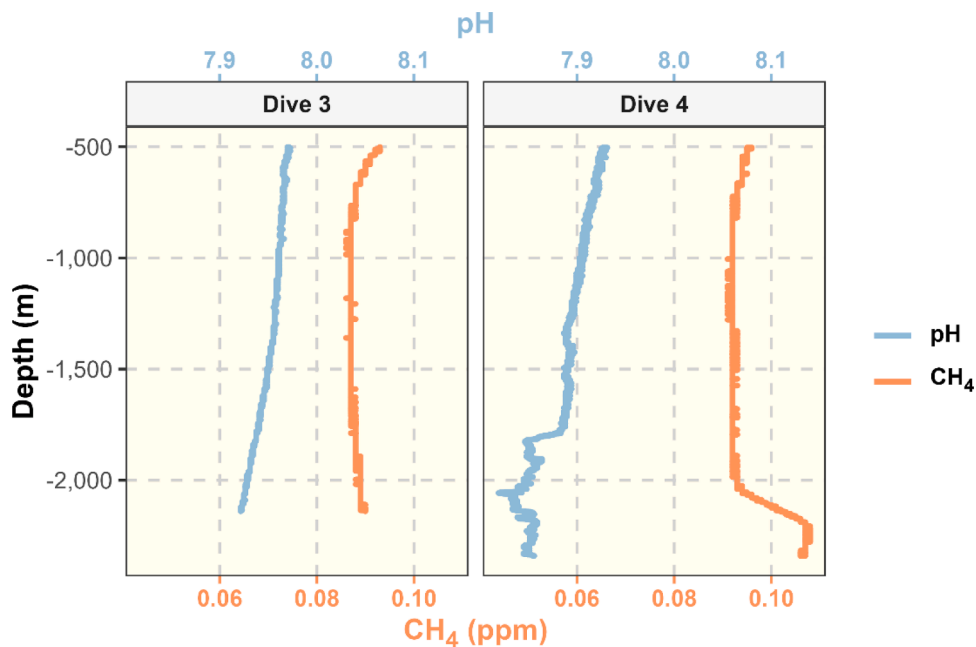


Fig. 5. Comparison of the depth profiles for pH and CH₄ for plume region dives 3 and 4. Note that the upper x-axis is for pH values, while the lower x-axis is for the CH₄ values.

inconsistent with biogenic degradation of organic matter. At the deeper parts of the Norwegian Sea, this Arctic water is characterized by a high content of inorganic carbon of around 2170–2190 μmol/kg, with somewhat lower values in the upper Atlantic water of ca. 2150–2160 μmol/kg (Jones et al., 2019). Previous monitoring of the Norwegian Sea has shown increasing pH with depth for the intermediate waters

between 750–2000 m depth, with a minimum in pH occurring in the lower part of the Atlantic waters at around 500–750 m depth (Jones et al., 2019).

A possible factor that may affect the pH-pO₂ correlation in Arctic water is its origin far north. Although the extent of primary production, i.e. the amount of organic production from photosynthesis, is largely

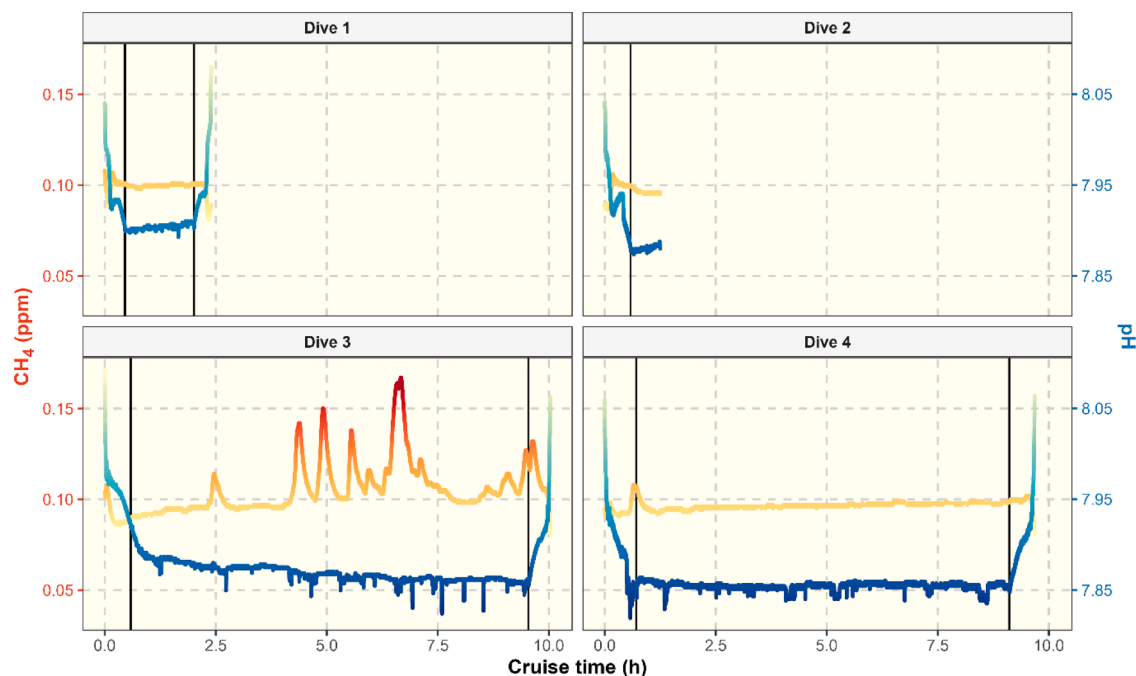


Fig. 6. Comparison of CH_4 and pH measurements during descent and bottom cruise for reference site dives 1 and 2 (top) and plume region dives 3 and 4 (bottom). Black vertical lines indicate the transition between descent and bottom cruise (left line) and bottom cruise and ascent (right line). Dive 2 was prematurely aborted because the AUV came too close to a seamount. Note that the left y-axis is for CH_4 , while the right y-axis is for pH.

unknown, the strong dependency upon availability of light and nutrients suggests that primary production is highly seasonal in the Arctic region. Lower irradiance is due to ice and snow coverage and the Polar Nights during winter months. Such factors may contribute to the observed vertical variations in pH and oxygen, which seem less dependent on biogenic respiration and degradation processes.

Moreover, at higher depths, increasing solubility of carbonates to bicarbonate will provide additional buffering of pH. This will also affect the vertical pH- pO_2 correlation since dissolution of carbonate affects pH, but not pO_2 . According to Jones et al. (2019) the aragonite compensation depth in the Norwegian Sea is located between 1500 and 2000 m depth. Hence, although this mechanism can have some effect on the observed pH- O_2 relationship at higher depths, it is unlikely to be the sole explanation for the pH- pO_2 observations in the Arctic water masses between ca. 670–1600 m, at the reference site.

At the hydrothermal vent site pO_2 and pH were well correlated at upper and intermediate depths. The stratification of the water column here indicates that these water masses are of a different origin compared to the reference site. The complete lack of correlation at lower depths may be attributed to the hydrothermal activity, which showed a significant lowering effect on pH while corresponding pO_2 levels were unaffected. Negative spikes in pH were detected as the AUV passed over the hydrothermal vent field, without corresponding negative spikes in pO_2 , which confirms that the pH reduction is caused by CO_2 from an abiotic source.

Small-scale experiments with artificial release of CO_2 to the water column have previously shown this effect in close vicinity to the leak (Blackford et al., 2017; Totland et al., 2020; Utchimoto et al., 2017, 2018). In contrast to such experiments, hydrothermal vent sites release comparably large amounts of CO_2 , and have been doing so for thousands of years. Hence, such vents offer the opportunity to study the effects of prolonged and extensive release of CO_2 to the water column, representing the far opposite end of the scale compared to artificial leakage scenarios.

Our data show that similar effects are seen in the water column in both cases, but at vastly different scales. Whereas small-scale CO_2 releases only affect a limited portion of the water column, the effects of

hydrothermal activity on the water column can be detected up to 700 m above the sea floor. The vertical distribution of these effects has not been studied but considering the slow circulation of the Norwegian Sea Deep Water it is possible that hydrothermal activity affects the chemical signature of a significant portion of this water mass.

In a previous study, we found very good correlation between pH and pO_2 at 60 m depth in the Oslo Fjord over four weeks, and clearly distinguishable deviations from this correlation caused by artificial non-biogenic CO_2 discharges (Totland et al., 2020). Another key difference between these studies is that sensors were mounted on stationary platforms on the Oslo Fjord seabed, whereas in the current study the parameters are monitored during the descent of the AUV vertically in the water masses. It is possible that a more complex environment requires a stationary sensor monitoring a single location over time to detect anomalous co-variation in pH and pO_2 due to leakage. Introduction of new water masses to the stationary sensors in the Oslo Fjord were followed by subtle changes in the pH- pO_2 correlation (Totland et al., 2020). However, since the sensors were stationary, the correlation was easy to detect despite exchange of water masses. If similar phenomena take place in the various water masses of the Norwegian Sea, data interpretation may be more complicated when sensors move vertically through the water masses on a mobile sensor platform such as an AUV.

Most plans to store CO_2 in offshore geological formations are currently focused on shallower shelf regions with water depths of <200 m. However, for CCS to significantly contribute to the IPCC strategy to restrict the global temperature increase to 1.5 °C, billions of tonnes of CO_2 must be stored annually. To achieve this, the number of offshore GCS sites must increase drastically. The trend in offshore petroleum activities has been to move to deeper waters over the past decades. For example, in the Gulf of Mexico, deepwater (>330 m) production had overtaken shelf production by 1999 (Sandrea and Stark, 2020), and in 2019 the Shell/GNOOC Appomattox field located at 2 250 m depths went on production. Similarly, as the search for suitable offshore geological formations for CO_2 storage progresses, offshore GCS may be focused on deeper waters in the future. The results of this study demonstrate that monitoring of deep sites may come with a different set of issues and complexities.

5. Conclusions

Our findings show an inverse pH-pO₂ relation for water originating from the Arctic Ocean, which is opposite to waters originating in the North Atlantic Ocean. Differences include a higher level of dissolved inorganic carbon in the Arctic waters compared to the Atlantic waters, as well as historical differences in biological activity, both of which may affect the pH-pO₂ correlation. This shows that results from previous studies regarding the pO₂-pH correlation are not always relevant when designing monitoring programs for other types of water masses. Depending on the history of that water mass, the correlation may be weaker or, like in the Arctic Waters investigated here, inverse.

Our results show that a priori knowledge of the chemical composition and correlations in the ocean may improve the planning and implementation of sensor systems for marine environmental monitoring. Several large-scale Carbon Capture and Storage projects are currently in the planning stage worldwide, which has spawned considerable research efforts towards monitoring of offshore storage reservoirs in recent years (Jenkins et al., 2015). One particular area of interest is how a potential CO₂ leak will affect the water column above the reservoir, and which chemical markers can be used to identify possible leaks (Blackford et al., 2017; Omar et al., 2021; Totland et al., 2020). The hydrothermal vent activity at Mohn's Ridge releases considerable amounts of CO₂ and understanding the effects of this large-scale natural CO₂ leakage on the surrounding waters can help understand how leakage from a geologic reservoir may affect the water column and how it may be detected by monitoring. This study shows that in deep waters, with very low exchange with adjacent water masses or the air-sea interface, large-scale CO₂ leakage affects a larger body of water. Hence, for CO₂ storage projects in such waters, chemical monitoring strategies may be different.

Moreover, the knowledge that pH-pO₂ correlations can potentially be naturally inverse in certain water masses means that a thorough characterization must be conducted of the water masses at a monitoring site before this correlation can be used to monitor for possible leakage.

Funding sources

This study was carried out as part of the ACT4storage project, funded through the CLIMIT program managed by Gassnova.

CRedit authorship contribution statement

Christian Totland: Conceptualization, Methodology, Formal analysis, Visualization, Writing – original draft. **Espen Eek:** Conceptualization, Methodology, Formal analysis, Writing – review & editing. **Raoul Wolf:** Formal analysis, Visualization, Writing – review & editing. **Ivar-Kristian Waarum:** Conceptualization, Data curation, Writing – review & editing. **Ann Elisabeth Albright Blomberg:** Conceptualization, Supervision, Project administration, Funding acquisition, Writing – review & editing.

Declaration of Competing Interest

The authors declare that they have no known competing financial interests or personal relationships that could have appeared to influence the work reported in this paper.

The authors declare the following financial interests/personal relationships which may be considered as potential competing interests:

Data availability

Data will be made available on request.

References

- Bickle, M.J., 2009. Geological carbon storage. *Nat. Geosci.* 2, 815.
- Blackford, J., Artioli, Y., Clark, J., de Mora, L., 2017. Monitoring of offshore geological carbon storage integrity: implications of natural variability in the marine system and the assessment of anomaly detection criteria. *Int. J. Greenh. Gas Control* 64, 99–112.
- Blindheim, J., 1985. Ecological features of the Norwegian Sea. *E. J. Drill*.
- Blindheim, J., 1990. Arctic intermediate water in the Norwegian sea. *Deep Sea Res. Part A Oceanogr. Res. Pap.* 37, 1475–1489.
- Burd, A., Frey, S., Cabre, A., Ito, T., Levine, N., Lønborg, C., Long, M., Mauritz, M., Thomas, Q., Stephens, B., Vanwallinghem, T., Zeng, N., 2015. Terrestrial and marine perspectives on modeling organic matter degradation pathways. *Glob. Change Biol.* 22.
- Caldeira, K., Wickett, M.E., 2005. Ocean model predictions of chemistry changes from carbon dioxide emissions to the atmosphere and ocean. *J. Geophys. Res. Oceans* 110.
- Dick, H.J.B., Lin, J., Schouten, H., 2003. An ultraslow-spreading class of ocean ridge. *Nature* 426, 405–412.
- Hawkes, J.A., Rossel, P.E., Stubbins, A., Butterfield, D., Connelly, D.P., Achterberg, E.P., Koschinsky, A., Chavagnac, V., Hansen, C.T., Bach, W., Dittmar, T., 2015. Efficient removal of recalcitrant deep-ocean dissolved organic matter during hydrothermal circulation. *Nat. Geosci.* 8, 856–860.
- Humphreys, M.P., Daniels, C.J., Wolf-Gladrow, D.A., Tyrrell, T., Achterberg, E.P., 2018. On the influence of marine biogeochemical processes over CO₂ exchange between the atmosphere and ocean. *Mar. Chem.* 199, 1–11.
- Jenkins, C., Chadwick, A., Hovorka, S.D., 2015. The state of the art in monitoring and verification – ten years on. *Int. J. Greenh. Gas Control* 40, 312–349.
- Jones, E., Chierici, M., Skjelvan, I., Norli, M., Børshheim, K.Y., Lødemel, H.H., Kutti, T., Sørensen, K., King, A.L., Lauvset, S., Jackson, K., Lange, T.d., Johannessen, T., Mourgue, C., 2019. Monitoring Ocean Acidification in Norwegian Seas in 2018. Institute of Marine Research, NORCE and University of Bergen. <https://www.miljo.direktoratet.no/globalassets/publikasjoner/m1417/m1417.pdf>.
- Lønborg, C., Carreira, C., Jickells, T., Alvarez-Salgado, X.A., 2020. Impacts of global change on ocean dissolved organic carbon (DOC) cycling. *Front. Mar. Sci.* 7.
- Martinez-Cabanas, M., Esposito, M., Gros, J., Linke, P., Schmidt, M., Triest, J., Achterberg, E.P., 2021. Deviations from environmental baseline: detection of subsea CO₂ release in the water column from real-time measurements at a potential offshore carbon dioxide storage site. *Int. J. Greenh. Gas Control* 109, 103369.
- Muggeo, V.M.R., 2003. Estimating regression models with unknown break-points. *Stat. Med.* 22 (19), 3055–3071. <https://doi.org/10.1002/sim.1545>.
- Muggeo, V.M.R., 2016. Testing with a nuisance parameter present only under the alternative: a score-based approach with application to segmented modelling. *J. Stat. Comput. Simul.* 86 (15), 3059–3067. <https://doi.org/10.1080/00949655.2016.1149855>.
- Muggeo, V.M.R., 2017. Interval estimation for the breakpoint in segmented regression: a smoothed score-based approach. *Aust. N. Z. J. Stat.* 59 (3), 311–322. <https://doi.org/10.1111/anzs.12200>.
- Ohtaki, E., Yamashita, E., Fujiwara, F., 1993. Carbon dioxide in surface seawaters of the Seto Inland Sea, Japan. *J. Oceanogr.* 49, 295–303.
- Omar, A.M., García-Ibáñez, M.I., Schaap, A., Oleynik, A., Esposito, M., Jeansson, E., Loucaides, S., Thomas, H., Alendal, G., 2021. Detection and quantification of CO₂ seepage in seawater using the stoichiometric Cseep method: results from a recent subsea CO₂ release experiment in the North Sea. *Int. J. Greenh. Gas Control* 108, 103310.
- Pedersen, R.B., Thorseth, I., Nygård, T., Lilley, M., Kelley, D., 2010a. Hydrothermal activity at the arctic mid-ocean ridges. *Washington DC Ame. Geophys. Union Geophys. Monogr. Ser.* 188, 67–89.
- Pedersen, R.B., Rapp, H.T., Thorseth, I.H., Lilley, M.D., Barriga, F.J.A.S., Baumberger, T., Flesland, K., Fonseca, R., Früh-Green, G.L., Jørgensen, S.L., 2010b. Discovery of a black smoker vent field and vent fauna at the Arctic Mid-Ocean Ridge. *Nat. Commun.* 1, 126.
- R Core Team, 2022. R: a Language and Environment for Statistical Computing. R Foundation for Statistical Computing, Vienna, Austria. URL: <https://www.R-project.org/>.
- Resing, J.A., Lupton, J.E., Feely, R.A., Lilley, M.D., 2004. CO₂ and 3He in hydrothermal plumes: implications for mid-ocean ridge CO₂ flux. *Earth. Planet. Sci. Lett.* 226, 449–464.
- Sandrea, R., Stark, P., 2020. Deepwater Oil Exploration in the Gulf of Mexico. A Spatial Model Provides Clues for Undiscovered Potential. *EPRINC*. July 2020.
- Siskin, M., Katritzky, A.R., 1991. Reactivity of organic compounds in hot water: geochemical and technological implications. *Science* 254, 231–237.
- Sprintall, J., Siedler, G., Mercier, H., 2013. Inter-ocean and interbasin exchanges. *Int. Geophys.* 103, 493–518.
- Swift, J.H., Koltermann, K.P., 1988. The origin of norwegian sea deep water. *J. Geophys. Res. Oceans* 93, 3563–3569.
- Totland, C., Eek, E., Blomberg, A.E.A., Waarum, I.K., Fietzek, P., Walta, A., 2020. The correlation between pO₂ and pCO₂ as a chemical marker for detection of offshore CO₂ leakage. *Int. J. Greenh. Gas Control* 99, 103085.
- Uchimoto, K., Kita, J., Xue, Z., 2017. A novel method to detect CO₂ leak in offshore storage: focusing on relationship between dissolved oxygen and partial pressure of CO₂ in the Sea. *Energy Proced.* 114, 3771–3777.
- Uchimoto, K., Nishimura, M., Kita, J., Xue, Z., 2018. Detecting CO₂ leakage at offshore storage sites using the covariance between the partial pressure of CO₂ and the saturation of dissolved oxygen in seawater. *Int. J. Greenh. Gas Control* 72, 130–137.
- Uchimoto, K., Watanabe, Y., Xue, Z., 2021. Seasonal dependence of false-positives in detection of anomalous pCO₂ using the covariance method with dissolved oxygen in monitoring offshore CO₂ storage sites. *Mar. Pollut. Bull.* 166, 112238.

Zeileis, A., Köll, S., Graham, N., 2020. Various versatile variances: an object-oriented implementation of clustered covariances in R. *J. Stat. Softw.* 95 (1), 1–36. <https://doi.org/10.18637/jss.v095.i01>.

Zeileis, A., 2004. Econometric computing with HC and HAC covariance matrix estimators. *J. Stat. Softw.* 11 (10), 1–17. <https://doi.org/10.18637/jss.v011.i10>.

Zeileis, A., 2006. Object-oriented computation of sandwich estimators. *J. Stat. Softw.* 16 (9) <https://doi.org/10.18637/jss.v016.i09>.